Biointerface Research in Applied Chemistry
Platinum Open Access Journal (ISSN: 2069-5837)

Article
Volume 10, Issue 5, 2020, 6354 - 6364
https://doi.org/10.33263/BRIAC105.63546364

Enhancement of Mercury Removal by Utilizing Catalytic Chelation Technique

Mubasher Furmuly [1,2], Faizuan Abdullah [1,*], Ihsan Wan Azelee [1], Razali Ismail [1], Fuaad Omar [1], Dedy Dwi Prastyo [3], Achmad Syafiuddin [4,*]

[1] Department of Chemistry, Faculty of Science, Universiti Teknologi Malaysia, 81310 UTM Johor Bahru, Johor, Malaysia
[2] Department of Analytical Chemistry, Faculty of Chemistry, Kabul University, Jamal Mina, Kabul, Afghanistan
[3] Department of Statistics, Faculty of Science and Data Analytics, Institut Teknologi Sepuluh Nopember, 60111 Surabaya, East Java, Indonesia
[4] Department of Water and Environmental Engineering, Faculty of Engineering, Universiti Teknologi Malaysia, 81310 UTM Johor Bahru, Johor, Malaysia
* Correspondence: faizuan@utm.my (F.A.); ac.syafi@gmail.com (A.S.);
Scopus Author ID 55053616200 (F.A.); 56682128000 (A.S.)
Received: 14.04.2020; Revised: 5.05.2020; Accepted: 6.05.2020; Published: 13.05.2020

Abstract: Discharge of heavy metals released from industries has adverse effects on the environment. The development of a method that can safely remove heavy metals is still challenging. Therefore, the aim of this study is to propose catalytic chelation technique for the removal of mercury (Hg). Removal of Hg was carried out using the sodium acetate (CH_3COONa) as the chelating agent and catalyzed by the heterogeneous alumina supported calcium oxide (CaO/Al_2O_3). The optimization was performed by applying the Response Surface Methodology (RSM) with the pH ranging from 7 to 10, a dosage of chelating agent from 400 ppm to 600 ppm, temperature from 33.5 to 37.5 ^oC, and time of reaction from 1 to 5 h. Hg content analysis was carried out using Flow Injection Mercury System based on cold vapor atomic absorption spectroscopy. X-ray diffraction (XRD) analysis revealed the presence of active sites on the catalyst. Field Emission Scanning Electron Microscopy (FESEM) analysis represented the formation of homogeneous particles on the catalyst surface. The Brunauer-Emmett-Teller (BET), Energy Dispersive X-Ray (EDX), and Fourier-transform Infrared Spectroscopy (FTIR) confirmed the surface area, the elemental composition, and functional groups of the catalyst, respectively. Moreover, the proposed method successfully achieved ±99 % of Hg removal.

Keywords: Mercury removal; chelation technique; catalyst; water pollution.

1. Introduction

Currently, the contaminated water becomes a major problem since Malaysia have concerned about industrial development [1-7]. A large amount of industrial pollutions containing poisonous chemicals especially heavy metals is released into water systems and are the main reason for seafood contamination by heavy metals [8-10]. The dosage of trace heavy metals in marine ecosystem is very low. However, some marine bivalves are capable of concentrating heavy metals in their tissues more than a million times compared to their concentration in the habitat [11]. Cockles are one of the marine mollusks which are widely consumed in Malaysia because it is easy to trap, a high biological value source of protein, vitamins, and minerals. They can be easily polluted by effluents coming from anthropogenic activities, sewage discharge, shipping activities, agricultural activities, and other contamination

sources. It is a big concern for humans because the heavy metals coming from industrial effluents or by natural means are harmful and even can be carcinogenic to human.

The cockles are exposed to heavy metals such as cadmium, lead, arsenin, and mercury. The metals are toxic even in small amounts and can affect the immune system, nervous system, and reproductive system. There are three categories of heavy metals, namely, potentially toxic (arsenic, cadmium, lead, and mercury), probably essential (nickel, vanadium, and cobalt) and essential (copper, zinc, iron, and manganese). Since cockles are filter feeder organisms, so there is a high possibility of contamination by heavy metals, which are potentially poisonous, especially mercury which is one of the most toxic heavy metals and classified as potentially toxic heavy metals [12].

Furthermore, mercury is considered as a major environmental pollutant, since mercury mainly exists as Hg^0 in the atmosphere which can stay there for a long period of time and can travel over a large geographical distance and can be absorbed by land or water [13]. As long as most of the accumulated mercury in trophic levels comes from dietary sources rather than from direct water intake, thus cockles as a filter feeder, consume phytoplankton at the bottom of the food chain which accumulates and transforms mercury from the environment [14]. Biotransformation of mercury species by marine phytoplankton is more important than the bioavailability of mercury in marine phytoplankton, in addition phytoplankton and other bacteria are able to reduce Hg(II) to volatile Hg^0 which makes a global health concern [15,16].

A number of methods and materials have been suggested for the removal of mercury from different environments [17-22]. For instance, high removal of mercury from chloralkali wastewater can be achieved by a biofilm of mercury-resistant bacteria [23]. Alternatively, the porous organic polymer-based mercury can effectively reduce the mercury (II) concentration from 10 ppm to a fairly low concentration of 0.4 ppm within a short period of time [24]. Of all the treatment techniques for the removal of heavy metals, the chelation technique is widely used as a treatment technique for the removal of heavy metals such as lead, mercury, and arsenic. Chelating agents such as ethylene diamine tetraacetic acid (EDTA), 2,3-dimercapto succinic acid (DMSA), and 2,3-dimercapto propansulfuric acid (DMPS) are used to bind heavy metals and excrete from the blood to urine. Moreover, chelation technique has been found to be a likely method for the removal of heavy metals to levels permissible by Malaysian food regulations.

In this work, we propose a catalytic chelation technique for the removal of mercury. This study provided an important opportunity to advance the understanding of the use of this technique for the removal of various heavy metals from the environment.

2. Materials and Methods

2.1. Materials.

Chemical and reagents of analytical grade have been used for this study and no purification has been done before using the chemicals. The chemicals were 65% Nitric acid, HNO_3 (QRëC™) and 30% Hydrogen peroxide, H_2O_2 (QRëC™) used for digestion, sodium acetate trihydrate, $CH_3COONa.3H_2O$ (MERCK) as a chelating agent, calcium oxide on alumina support (CaO/Al_2O_3) as a catalyst, 0.05% Sodium hydroxide + Sodium borohydride as a reductant, $NaOH+NaBH_4$ (QRëC™), 3% HCl (QRëC™) as a carrier, 5% $KMnO_4$, potassium permanganate for mercury samples, 10% HCl for preparation of solutions, 1000 ppm

mercury (Hg) stock solution (MERCK) for preparing mercury standard solutions. Ultra-pure water from a NANO pure water system has been used for all dilution purposes.

2.2. Sample preparation.

The *Anadara granosa* was purchased from a fisherman at Pontian, Johor Bahru, Malaysia and then transported to the analytical laboratory of Universiti Technologi Malaysia inside the ice boxes at a temperature of 4^{o} C to avoid thermal degradation and microbial activity and acidified with concentrated nitric acid to pH <2. Prior to removing the soft tissues of the cockles from its outer shell, the shell surface was washed with tap water to remove the specks of dirt and other contaminating organisms such as barnacles and bryzoa, then the samples were grounded and homogenized using a mixer and refrigerated at -10^{o} C for further treatment. Sample preparation was done according to the nitric acid digestion method adopted from Association of Official Agricultural Chemists (AOAC 999.10). In the preparation, a 0.5g of the cockles was weighed into a digestion vessel and 5 mL of analytical grade 65% HNO_3 (w/w) and 2 mL of 30% H_2O_2 (w/w) was added into the sample and then the digestion was conducted by the aid of a Microwave digester (Perkin Elmer Titan MPS™) until a clear solution of the sample was produced. The sample was allowed to cool and then volumized with 25 mL of ultrapure water, 1-2 drops of $KMnO_4$ was added to the samples in order to convert organically bound mercury to inorganic mercury ions at room temperature [25].

2.3. Preparation of catalyst.

Calcium nitrate tetrahydrate powder was prepared by mixing 5 g of it into the 5 mL of deionized water in a beaker (250 mL), then the mixture was heated and stirred until the complete dissolve of the powder and the mixture was allowed to cool to room temperature. The alumina pellets were immersed into the solution and left for an hour at room temperature before calcined in a muffle furnace at 900 ^{o}C, 1000 ^{o}C, and 1100 ^{o}C. Next, the pellets were aged at 80^{0}C for 24 hours, and then calcined for 5 hours to prepare the proposed catalyst.

2.4. Mercury removal.

The flesh of the cockles was washed with deionized water after removing from its shell and then exposed to treatment with the chelating agent inside a 250 mL beaker, where the flesh was held inside the beaker with the aid of a string, and the solution was stirred using IKA HS-7 magnetic stirrer during the treatment process. The treatment was done using different dosage of chelating agent (200 to 600 µL/L), with the treatment temperature of (32.50±0.50 ^{o}C to 37.50±0.50 ^{o}C), treatment time ranging from 1 hour to 5 hours and pH ranging from acidic (pH = 4) to basic (pH = 10) in order to obtain the optimized condition for the highest percentage removal of mercury from cockles. CaO/Al_2O_3 was used as a catalyst during the treatment process and a 0.25 g of it was left in the beaker containing the chelating agent solution and was stirred throughout the treatment process. Each experiment was done with a replicate of three times in order to get the mean value and standard deviation concentration of the mercury inside the cockles.

2.5. Fourier transforms infrared spectroscopy analysis.

A Perkin Elmer flow-injection mercury system (FIMS-100) was used for the analysis of mercury content in the treated cockles, which is based on the cold vapor atomic absorption

spectroscopy and contains a single peristaltic pump, elevated optics, low-pressure mercury lamp, and a solar-blind detector for high sensitivity. An auto-sampler injected the sample into the system and an acid carrier was used for transporting the sample to the mixing section. Next, the sample was mixed with the reductant and a vapor hydride of mercury was produced during the reaction which was purged by the aid of argon with a regulate pressure to the gas-liquid separator and was then carried to the FIMS cell for detection by the help of mercury lamp.

Sodium borohydride ($NaBH_4$) was used as a reductant which was prepared from a 0.05% solution of sodium hydroxide (NaOH) and 0.2% sodium borohydride ($NaBH_4$). Hydrochloric acid, (3% HCl) was used as the carrier and prepared by diluting the concentrated HCl. A solution of 5% $KMnO_4$ was added to the digested samples. In order to prepare the standard solutions to plot the calibration curve, the 1000 ppm mercury stock solution (MERCK) was used to make a 10 ppm mercury as an intermediate stock solution then the standard series was made with the concentration of 1 ppb, 2 ppb, 5 ppb, and 10 ppb with quality control of 6 ppb into a 25 mL volumetric flask.

2.6. Optimization of mercury removal.

For the optimization purpose, the Box-Behnken design of Response Surface Methodology (RSM) was employed by multiple regression analysis [26-28]. The independent variables of this study were, the dosage of chelating agent (A), time of treatment (B), temperature (C), and pH of the solution (D). Table 1 shows the levels of each factor based on RSM approach. In the Design Expert, an equation is used in order to approximate the optimum value and determine the interaction between the variables, and a quadratic equation model was employed in this work.

Table 1. Experimental design for the mercury removal.

Factors	Symbols	Units	Range and levels		
			-1	0	+1
Dosage	A	mg/L	400	500	600
Time	B	h	1	3	5
Temperature	C	°C	29.5	32.5	37.5
pH	D		4	7	10

2.7. Characterization.

In order to determine the active site of catalyst for enhancement of mercury depuration from cockles, the characterization was performed utilizing analytical techniques such as X-Ray Diffraction (XRD) using A Bru-ker AXS D8 automatic powder diffractometer, Field Emission Scanning Electron Microscopy (FESEM) using Zeiss Supra 35VP model, Energy Dispersion X-Ray (EDX), Nitrogen Absorption (BET surface area) using a Micromeritics 3flex instrument, and Fourier Transform Infrared Spectroscopy (FTIR) using a Thermo Nicolet-iS10 spectrometer. The characterizations were presented for the next section.

3. Results and Discussion

3.1. Mercury removal.

The regression model obtained from RSM study is graphically displayed by 3-dimensional contour plots to illustrate the interactive effect of factors on the removal percentage of mercury from cockles. The 3-dimensional contour plots are displayed in Figure 1. The time of treatment combined with concentration has a significant interactive effect on

percentage removal of mercury by a removal percentage of (±95%), at a concentration of 500 mg/L and 1 hour of treatment. The increasing of time of treatment from 1 hour to 5 hours does not influence the removal of mercury as the increase of concentration.

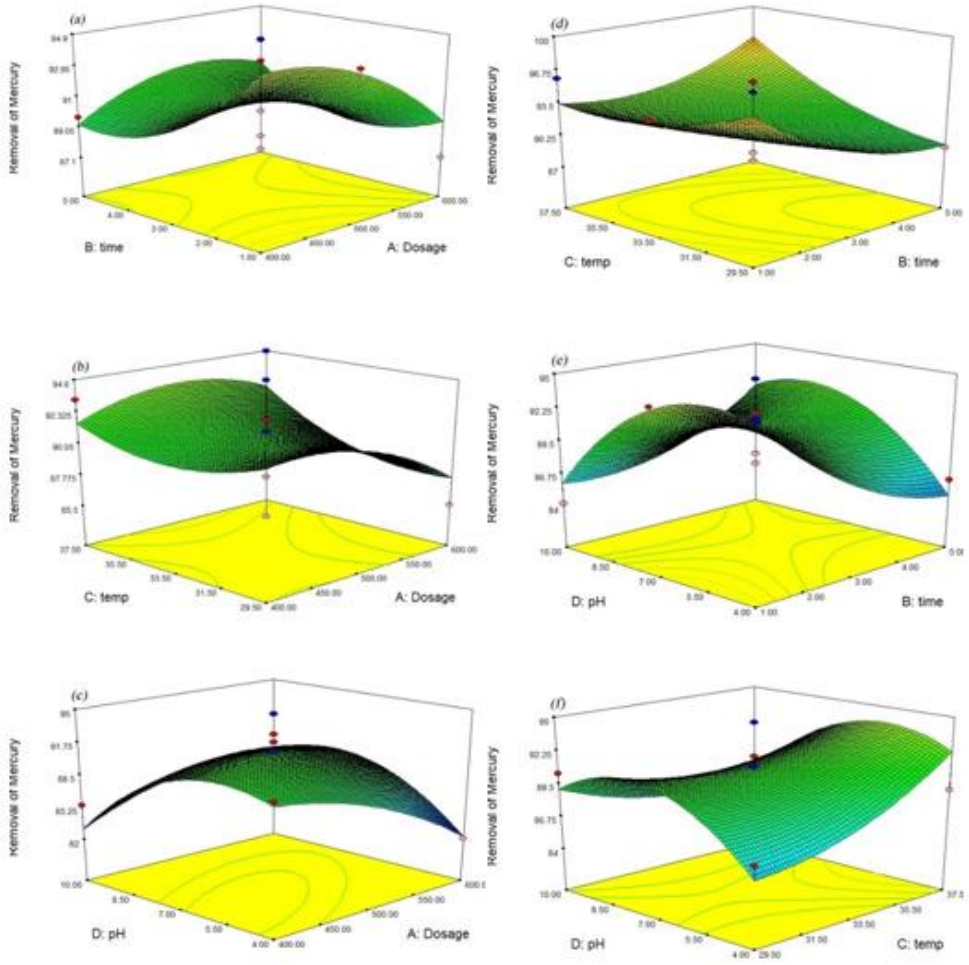

Figure 1. Three-dimensional contour plots for removal of mercury for (a) AB (b) AC (c) AD (d) BC (e) BD (f) CD. It is noted that A, B, C, and D are dosage of chelating agent, time of treatment, temperature, and pH of the solution, respectively.

The time of treatment combined with the temperature is another significant interaction with a percentage removal of (±99%). The increase in both variables did not influence the removal percentage of mercury and was maximum at temperature 29.5 ^{o}C and treatment time of 1 hour. Furthermore, the combination of pH and time of treatment also has a remarkable role on the removal of mercury with a percentage of (±94%) at pH of 7 and 1 hours of treatment. The removal percentage increases with increment of pH of the solution from acidic (pH 4) to neutral media (pH 7), meanwhile, the increasing time of treatment has not a significant role in percentage removal of mercury compared to the pH of the solution. The present study revealed an improved performance compared to previous studies in terms of percentage removal. For instance, the removal of mercury using activated carbons derived from organic sewage sludge can only be achieved by up to 83% [29]. Alternatively, the maximum mercury removal by nonviable biomass of an estuarine *Bacillus* sp. was by 92% [30].

3.2. XRD analysis.

In order to investigate the crystallinity of CaO/Al_2O_3, XRD analysis was performed and the data obtained from the analysis is presented in Figure 2. It is noted from the figure that the

catalyst calcined at 900 ºC has a broad amorphous pattern which represents a low degree of crystallinity in the catalyst. According to the diffractogram, $Al_{2.66}O_4$ is the only alumina support species which is present in cubic phase at 2θ = 67.181°, 45.832° and 37.435°, while none of the active metal species are present at this calcination temperature. The CaO/Al_2O_3 calcined at 1000 ºC represents a high degree of crystallinity based on the sharp peaks in diffractograms, furthermore, orthorhombic Al_2O_3, monoclinic $CaAl_4O_7/CaO.2Al_2O_3$, and cubic $Ca_{12}Al_{14}O_{33}$ are three new species which were present at this calcination temperature which was revealed at 2θ = 67.354°, 66.767°, 45.881°, 45.407°, 34.554° and 36.568° for orthorhombic Al_2O_3. However, due to the solid state reaction, there are another two phases which noticed at 2θ = 25.494°, 34.554°, 19.990°, 28.989°, 30.528° and 33.032° for monoclinic $CaAl_4O_7/CaO.2Al_2O_3$ while at 2θ = 18.412°, 33.427° and 36.568° for cubic $Ca_{12}Al_{14}O_{33}$.

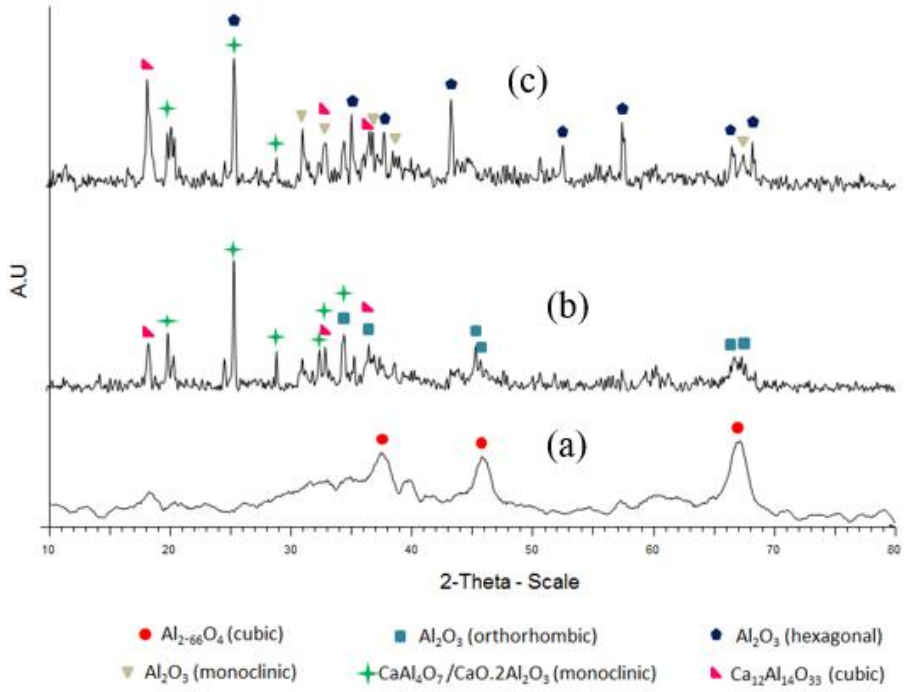

Figure 2. XRD Diffractograms of CaO/Al_2O_3 at different temperatures at (a) 900ºC, (b) 1000ºC, and (c) 1100 ºC.

At the calcination temperature of 1100 ºC, the peaks were observed to be even more intense compared to the calcination temperature at 1000 ºC. The dominated phase by alumina support was increased into two phases which were different from those in 1000 °C calcination temperature and presented as monoclinic and hexagonal Al_2O_3 that happened at 2θ = 67.411°, 31.119°, 32.980°, 36.841°, 38.858° and 2θ = 35.134°, 43.353°, 57.583°, 25.466°, 37.837°, 52.577°, 68.192°, and 66.480º, respectively, as listed in Table 2. Similarly, monoclinic $CaAl_4O_7/CaO.2Al_2O_3$ and cubic $Ca_{12}Al_{14}O_{33}$ species also occurred at 2θ = 18.316°, 33.419°, 36.625° and 2θ = 18.316°, 33.419°, and 36.625°, respectively.

The data obtained from the experiment involving CaO/Al_2O_3 catalyst at different calcination temperatures are presented in Table 2. It demonstrates that the higher catalytic activity occurred at 1000 ºC calcination temperature. It could be determined from the orthorhombic Al_2O_3 support which has the best alumina phase for the active species and there are other active site species in monoclinic $CaAl_4O_7/CaO.2Al_2O_3$ and cubic $Ca_{12}Al_{14}O_{33}$ phases as well. Furthermore, when the calcination temperature increased from 900 ºC to 1000 ºC, the

presence of active species also increased which was proven by the high crystallinity of the catalyst.

Table 2. Peaks assignment in the X-ray diffraction patterns of CaO/Al_2O_3 calcined at different temperatures.

Catalyst	2θ	d (Å)	$d (Å)_{ref}$
Calcined at 900˚C	67.181	1.392	1.400
	45.832	1.978	1.980
$Al_{2.66}O_4$ (c)	37.435	2.400	2.390
Calcined at 1000˚C	67.354	1.389	1.391
	66.767	1.400	1.405
Al_2O_3 (or)	45.407	1.996	1.990
	45.881	1.976	1.983
	34.554	2.594	2.596
	36.568	2.455	2.457
$CaAl_4O_7/CaO.2Al_2O_3$ (m)	25.494	3.491	3.500
	34.554	2.594	2.599
	19.990	4.815	4.440
	28.989	3.078	3.080
	32.528	2.750	2.753
	33.032	2.710	2.712
	18.412	4.815	4.891
$Ca_{12}Al_{14}O_{33}$ (c)	33.427	2.678	2.679
	36.568	2.455	2.445
Calcined at 1100˚C	25.466	3.495	3.500
	34.536	2.595	2.599
$CaAl_4O_7/CaO.2Al_2O_3$ (m)	19.990	4.438	4.440
	18.316	4.840	4.891
$Ca_{12}Al_{14}O_{33}$ (c)	33.419	2.679	2.679
	36.841	2.437	2.445
	67.411	1.388	1.380
Al_2O_3 (m)	31.119	2.872	2.801
	32.980	2.714	2.713
	36.841	2.438	2.441
	38.858	2.316	2.310
	35.134	2.552	2.552
Al_2O_3 (h)	43.353	2.085	2.086
	57.583	1.599	1.602
	25.466	3.494	3.481
	37.837	2.376	2.380
	52.577	1.739	1.741
	68.192	1.374	1.374
	66.480	1.405	1.405

3.3. Surface morphology.

The morphology of the catalyst (CaO/Al_2O_3) was observed by FESEM, where the active area of the catalyst was determined by the formation of morphology on the surface of the catalyst which is contributed to the enhancement of mercury depuration from cockles. The FESEM micrographs of CaO/Al_2O_3 catalyst calcined at 900 ^oC, 1000^0C, 1100^0C were presented in Figure 3. It is demonstrated that the catalyst has aggregation and agglomeration on the surface. The particles are not dispersed on the catalyst surface and have unspecific shape. In addition, the formation of particles with undefined shape, aggregation and agglomeration on its surface can be observed for the catalyst calcined at 1000 °C calcination temperature. At 1100 °C calcination temperature, the particles have large aggregation and agglomeration but less dense and dispersed.

At 1000 °C calcination temperature, highly dispersed particles were formed on CaO/Al_2O_3 catalyst. The catalyst surface was not homogenized at 900 ^oC due to a low degree of crystallinity according to the XRD results, meanwhile, the catalyst has a disordered structure at 1100 °C calcination temperature which is due to the presence of two alumina support species on the catalyst surface according to the XRD results. Thus, it can be observed from the FESEM

results that the CaO/Al_2O_3 catalyst calcined at 1000 °C has the characteristics which are the reason for the high catalytic activity of CaO/Al_2O_3 catalyst.

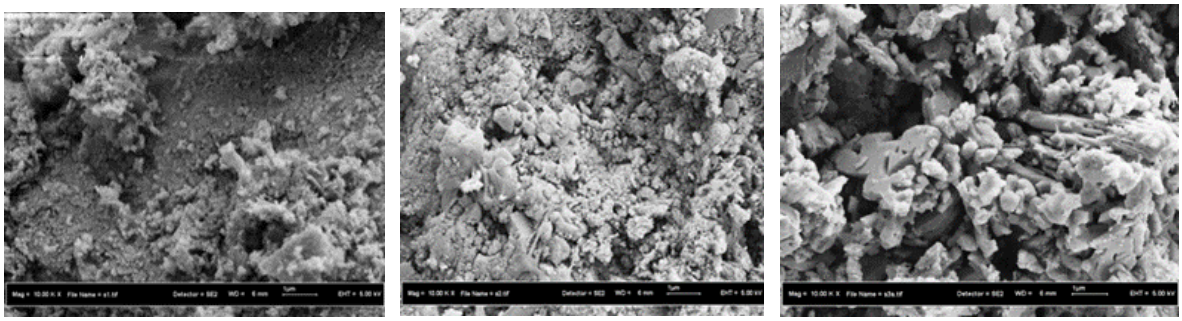

(a) (b) (c)

Figure 3. FESEM images of CaO/Al_2O_3 catalyst calcined at (a) 900°C, (b) 1000°C, and (c) 1100°C with magnification of 10000X.

3.4. Nitrogen adsorption analysis.

BET surface area analysis was performed to determine the surface area of the catalyst at different calcination temperatures as presented in Table 3 which demonstrates that the surface area of the catalyst is inversely proportional to the calcination temperature. It is in accordance with the XRD analysis representing an increase in the degree of crystallinity of catalyst decreased the surface area. The catalyst calcined at 1100 ^oC gave a low surface area (11.54 m^2/g) which is probably due to the large agglomeration and aggregation as described in FESEM analysis but regarding the catalytic activity results, catalyst calcined at 1000 °C showed the highest mercury removal which represents that the surface area parameter is not the only main factor for the mercury removal.

Table 3. BET surface area of CaO/Al_2O_3 catalyst calcined at different temperatures

Catalyst	Calcination temperature	Surface area (m^2/g)
CaO/Al_2O_3	900°C	68.16
	1000°C	33.22
	1100°C	11.54

3.5. EDX analysis.

The composition of the element which has distributed and coated on the alumina support was analysed by EDX and the results are shown in Table 4. This study found that the presence of O, Al, and Ca was confirmed by the EDX analysis and the weight percentage of Al and O is higher than the Ca due to the presence of Al_2O_3 support for the catalyst.

Table 4. EDX Analysis of CaO/Al_2O_3 catalyst calcined at different temperatures

Catalyst	Percentage (%)		
	O	Al	Ca
900 °C	61.52	32.45	6.03
1000 °C	57.43	35.93	6.64
1100 °C	49.76	43.04	7.20

3.6. FTIR analysis.

The FTIR spectra of CaO/Al_2O_3 catalyst calcined at different calcination temperatures are represented in Figure 4. The absorption bands between 579.02 to 811.18 cm^{-1} for CaO/Al_2O_3 catalysts were due to the stretching mode of metal oxide (M=O) groups. Accordingly, the wavelength at 1420.97 cm^{-1} for the catalysts calcined at 1000^0C and 1100^0C

indicates that the nitrate group in the catalyst had been completely removed, while the wavelength at 3436.38 cm^{-1} demonstrates the presence of H_2O stretching group.

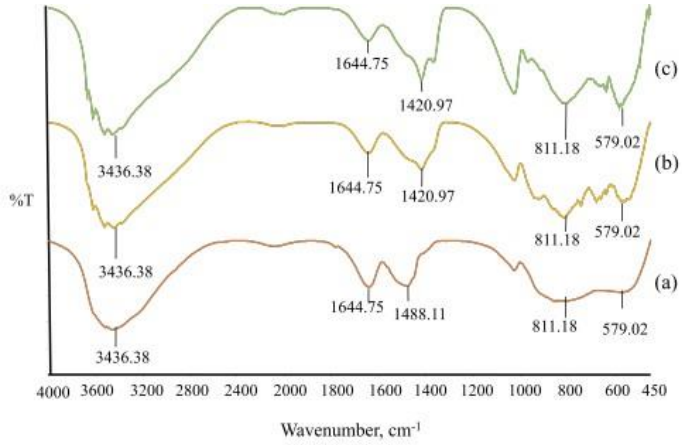

Figure 4. FTIR spectra of CaO/Al_2O_3 catalyst calcined at (a) 900°C, (b) 1000°C and (c) 1100°C.

4. Conclusions

The present study aimed to propose a chelation technique for the removal of Hg. RSM study revealed that the combined variables show a significant influence on percentage removal of mercury, which time of treatment and concentration had a significant interactive effect on percentage removal of mercury by a removal percentage of (±95%), at a concentration of 500 mg/L and 1 hour of treatment. Time of treatment combined with the temperature was another significant interaction with a percentage removal of (±99%) and the combination of pH and time of treatment also had a remarkable role on the removal of mercury with a percentage of (±94%) at pH of 7 and 1 hour of treatment. CaO/Al_2O_3 catalyst calcined at 1000 °C has remarkable performance because of its large surface area and presence of actives sites on catalyst confirmed by the XRD, FESEM, BET surface area, and EDX analyses.

Funding

This research was funded by the Universiti Teknologi Malaysia, grant number Q.J130000.2522.00H90.

Acknowledgments

The authors thank the Universiti Teknologi Malaysia for facilitating the research work.

Conflicts of Interest

The authors declare no conflict of interest.

References

1. Al Farraj, D.A.; Hadibarata, T.; Yuniarto, A.; Syafiuddin, A.; Surtikanti, H.K.; Elshikh, M.S.; Al Khulaifi, M.M.; Al-Kufaidy, R. Characterization of pyrene and chrysene degradation by halophilic Hortaea sp. B15. *Bioprocess and Biosystems Engineering* **2019**, *42*, 963-969, https://doi.org/10.1007/s00449-019-02096-8.
2. Hadibarata, T.; Syafiuddin, A.; Al-Dhabaan, F.A.; Elshikh, M.S.; Rubiyatno. Biodegradation of Mordant orange-1 using newly isolated strain Trichoderma harzianum RY44 and its metabolite appraisal. *Bioprocess and Biosystems Engineering* **2018**, *41*, 621-632, https://doi.org/10.1007/s00449-018-1897-0.
3. Syafiuddin, A.; Salmiati, S.; Jonbi, J.; Fulazzaky, M.A. Application of the kinetic and isotherm models for better understanding of the behaviors of silver nanoparticles adsorption onto different adsorbents. *Journal of Environmental Management* **2018**, *218*, 59-70, https://doi.org/10.1016/j.jenvman.2018.03.066.

4. Syafiuddin, A.; Hadibarata, T.; Zon, N.F.; Salmiati. Characterization of titanium dioxide doped with nitrogen and sulfur and its photocatalytic appraisal for degradation of phenol and methylene blue. *Journal of the Chinese Chemical Society* **2017**, *64*, 1333-1339, https://doi.org/10.1002/jccs.201700136.
5. Hadibarata, T.; Syafiuddin, A.; Ghfar, A.A. Abundance and distribution of polycyclic aromatic hydrocarbons (PAHs) in sediments of the Mahakam River. *Marine Pollution Bulletin* **2019**, *149*, https://doi.org/10.1016/j.marpolbul.2019.110650.
6. Syafiuddin, A.; Fulazzaky, M.A.; Salmiati, S.; Kueh, A.B.H.; Fulazzaky, M.; Salim, M.R. Silver nanoparticles adsorption by the synthetic and natural adsorbent materials: an exclusive review. *Nanotechnology for Environmental Engineering* **2020**, *5*, 1-18, https://doi.org/10.1007/s41204-019-0065-3.
7. Syafiuddin, A.; Salmiati, S.; Hadibarata, T.; Salim, M.R.; Kueh, A.B.H.; Suhartono, S. Removal of silver nanoparticles from water environment: Experimental, mathematical formulation, and cost analysis. *Water, Air, and Soil Pollution* **2019**, *230*, 102-117, https://doi.org/10.1007/s11270-019-4143-8.
8. Alkarkhi, F.A.; Ismail, N.; Easa, A.M. Assessment of arsenic and heavy metal contents in cockles (Anadara granosa) using multivariate statistical techniques. *Journal of Hazardous Materials* **2008**, *150*, 783-789, https://doi.org/10.1016/j.jhazmat.2007.05.035.
9. Syafiuddin, A.; Salmiati, S.; Salim, M.R.; Kueh, A.B.H.; Hadibarata, T.; Nur, H. A review of silver nanoparticles: Research trends, global consumption, synthesis, properties, and future challenges. *Journal of the Chinese Chemical Society* **2017**, *64*, 732-756, https://doi.org/10.1002/jccs.201700067.
10. Syafiuddin, A. Toward a comprehensive understanding of textiles functionalized with silver nanoparticles. *Journal of the Chinese Chemical Society* **2019**, *66*, 793-814, https://doi.org/10.1002/jccs.201800474.
11. Kahle, J.; Zauke, G.P. Bioaccumulation of trace metals in the calanoid copepod Metridia gerlachei from the Weddell Sea (Antarctica). *Science of the Total Environment* **2002**, *295*, 1-16, https://doi.org/10.1016/S0048-9697(01)01147-0.
12. Pradit, S.; Shazili, N.A.M.; Towatana, P.; Saengmanee, W. Accumulation of trace metals in Anadara granosa and Anadara inaequivalvis from Pattani Bay and the Setiu Wetlands. *Bulletin of Environmental Contamination and Toxicology* **2016**, *96*, 472-477, https://doi.org/10.1007/s00128-015-1717-z.
13. Wu, Y.; Wang, W.X. Accumulation, subcellular distribution and toxicity of inorganic mercury and methylmercury in marine phytoplankton. *Environmental Pollution* **2011**, *159*, 3097-3105, https://doi.org/10.1016/j.envpol.2011.04.012.
14. Wang, W.X.; Wong, R.S. Bioaccumulation kinetics and exposure pathways of inorganic mercury and methylmercury in a marine fish, the sweetlips Plectorhinchus gibbosus. *Marine Ecology Progress Series* **2003**, *261*, 257-268, https://doi.org/10.3354/meps261257.
15. Fantozzi, L.; Ferrara, R.; Frontini, F.P.; Dini, F. Dissolved gaseous mercury production in the dark: evidence for the fundamental role of bacteria in different types of Mediterranean water bodies. *Science of the Total Environment* **2009**, *407*, 917-924, https://doi.org/10.1016/j.scitotenv.2008.09.014.
16. Wu, Y.; Wang, W.X. Intracellular speciation and transformation of inorganic mercury in marine phytoplankton. *Aquatic Toxicology* **2014**, *148*, 122-129, https://doi.org/10.1016/j.aquatox.2014.01.005.
17. Johs, A.; Eller, V.A.; Mehlhorn, T.L.; Brooks, S.C.; Harper, D.P.; Mayes, M.A.; Pierce, E.M.; Peterson, M.J. Dissolved organic matter reduces the effectiveness of sorbents for mercury removal. *Science of the Total Environment* **2019**, *690*, 410-416, https://doi.org/10.1016/j.scitotenv.2019.07.001.
18. Jampaiah, D.; Chalkidis, A.; Sabri, Y.M.; Mayes, E.L.H.; Reddy, B.M.; Bhargava, S.K. Low-temperature elemental mercury removal over TiO2 nanorods-supported MnOx-FeOx-CrOx. *Catalysis Today* **2019**, *324*, 174-182, https://doi.org/10.1016/j.cattod.2018.11.049.
19. Qin, H.; He, P.; Wu, J.; Chen, N. Theoretical study of hydrocarbon functional groups on elemental mercury adsorption on carbonaceous surface. *Chemical Engineering Journal* **2020**, *380*, https://doi.org/10.1016/j.cej.2019.122505.
20. Ahmad, M.; Wang, J.; Xu, J.; Yang, Z.; Zhang, Q.; Zhang, B. Novel synthetic method for magnetic sulphonated tubular trap for efficient mercury removal from wastewater. *Journal of Colloid and Interface Science* **2020**, *565*, 523-535, https://doi.org/10.1016/j.jcis.2020.01.024.
21. An, D.; Sun, X.; Cheng, X.; Cui, L.; Zhang, X.; Zhao, Y.; Dong, Y. Investigation on mercury removal and recovery based on enhanced adsorption by activated coke. *Journal of Hazardous Materials* **2020**, *384*, https://doi.org/10.1016/j.jhazmat.2019.121354.
22. Hao, R.; Wang, Z.; Mao, X.; Gong, Y.; Yuan, B.; Zhao, Y.; Tian, B.; Qi, M. Elemental mercury removal by a novel advanced oxidation process of ultraviolet/chlorite-ammonia: Mechanism and kinetics. *Journal of Hazardous Materials* **2019**, *374*, 120-128, https://doi.org/10.1016/j.jhazmat.2019.03.134.
23. Von Canstein, H.; Li, Y.; Timmis, K.; Deckwer, W.D.; Wagner-Döbler, I. Removal of mercury from chloralkali electrolysis wastewater by a mercury-resistant Pseudomonas putida strain. *Applied and Environmental Microbiology* **1999**, *65*, 5279-5284, https://doi.org/10.1128/AEM.65.12.5279-5284.1999.
24. Li, B.; Zhang, Y.; Ma, D.; Shi, Z.; Ma, S. Mercury nano-trap for effective and efficient removal of mercury (II) from aqueous solution. *Nature Communications* **2014**. *5*, 5537, https://doi.org/10.1038/ncomms6537.
25. Guo, T.z.; Baasner, J.; Gradl, M.; Kistner, A. Determination of mercury in saliva with a flow-injection system. *Analytica Chimica Acta* **1996**, *320*, 171-176, https://doi.org/10.1016/0003-2670(95)00459-9.

26. Topal, M.; Arslan Topal, E.I. Optimization of tetracycline removal with chitosan obtained from mussel shells using RSM. *Journal of Industrial and Engineering Chemistry* **2020**, *1*, https://doi.org/10.1016/j.jiec.2020.01.013.
27. Gadekar, M.R.; Ahammed, M.M. Modelling dye removal by adsorption onto water treatment residuals using combined response surface methodology-artificial neural network approach. *Journal of Environmental Management* **2019**, *231*, 241-248, https://doi.org/10.1016/j.jenvman.2018.10.017.
28. Galedari, M.; Mehdipour Ghazi, M.; Rashid Mirmasoomi, S. Photocatalytic process for the tetracycline removal under visible light: Presenting a degradation model and optimization using response surface methodology (RSM). *Chemical Engineering Research and Design* **2019**, *145*, 323-333, https://doi.org/10.1016/j.cherd.2019.03.031.
29. Zhang, F.-S.; Nriagu, J.O.; Itoh, H. Mercury removal from water using activated carbons derived from organic sewage sludge. *Water Research* **2005**, *39*, 389-395, https://doi.org/10.1016/j.watres.2004.09.027.
30. Green-Ruiz, C. Mercury(II) removal from aqueous solutions by nonviable Bacillus sp. from a tropical estuary. *Bioresource Technology* **2006**, *97*, 1907-1911, https://doi.org/10.1016/j.biortech.2005.08.014.